Convective System Observations by LEO and GEO Satellites in Combination

Tran Vu La, *Member, IEEE*, and Christophe Messager

***Abstract*—The combination of low earth orbit (LEO) and GEO stationary (GEO) satellites brings significant advantages to observe, monitor, and understand convective systems and the associated vertical and horizontal dynamics. Two LEO, C-band Sentinel-1 synthetic aperture radar and *L*-band soil moisture active passive (SMAP) radiometer, are used to observe surface wind patterns, while the other LEO (Aeolus lidar instrument) offers the measurements of intense convective downdrafts. Meteosat GEO is used to detect deep convective clouds. Four case study examples of LEO and GEO combination illustrate here the matching in location and observation time between deep convective clouds, intense downdrafts, and strong surface wind gusts. In particular, the two-dimensional deep convective cloud patterns and surface wind patterns have the same direction displacement. The observations of surface wind patterns by two different LEO (Sentinel-1 and SMAP) indicate that the high-intensity radar backscattering on Sentinel-1 images should be induced by convective wind gusts rather than hydrometeors or convective precipitation at the sea surface as suggested in previous references. Finally, the convective wind gusts estimated from Sentinel-1 and SMAP data correspond to those obtained by the high-frequency radars, small-scale numerical models, and in-situ measurements.**

***Index Terms*—Aeolus, convective downdraft, convective wind gust, deep convection, geostationary (GEO), low earth orbit (LEO), Meteosat, Sentinel-1, soil moisture active passive (SMAP).**

I. Introduction

A CONVECTIVE system (CS) characterized by a cumulonimbus cloud (sometimes called storm) is an atmospheric feature where the atmosphere exhibits vertical displacements with some persistent upward and downward air fluxes, mutually connected by air parcel energy exchanges over a limited region around the cell. Indeed, the lower part of the atmosphere is destabilized by an energy input (warm air generated by solar radiation and/or surface heating), and then the density of the lower air parcel is modified. When an upward displacement is actually generated, that triggers the vertical convective instability. The upward movement (so-called updraft) is counterbalanced by a downward air current (so-called downdraft) after air parcel cooling at a higher altitude (see Fig. 1). These density differences result in rising and (or) falling currents, which are the key characteristics of a convection cell. These atmospheric dynamics may generate turbulence and strong wind even near the surface. The scale of such feature may vary from hundreds of meters (submesoscale) up to several kilometers and tens of kilometers when organized on a larger scale than the individual cells but smaller than extratropical cyclones and generally persists for several hours or more.

The CSs are the major issues for both extra-tropical and tropical regions since they are particularly intense and dangerous over the tropics (the Gulf of Guinea, the Gulf of Mexico, Lake Victoria, whole Southeast Asia, India, etc.), with the combination of heavy rainfall, surface wind gust, and intense lightning [1]–[5]. The CS observation and monitoring were improved in recent years [6]–[8], while the CS forecast is still a significant issue for the numerical weather prediction (NWP) models. Indeed, thanks to a quite complete network of geostationary (GEO) satellites, including Meteosat, GOES, Himawari, and Gaofen, one can observe and monitor CSs over Europe and Africa, America, and the Asia Pacific, respectively. The CS and deep convection may be associated with and detected by the coldest parts of the high-altitude tropospheric clouds. The convection is then called deep convection since it reaches high altitude and thus, the associated air parcel is dramatically cooled which leads to a resulting powerful descending air parcel. One can now observe and monitor CSs almost anywhere with a short time sampling frequency (up to only five minutes for the new generation of GEO satellites [9], [10]). However, the direct and remote observation of the CS effects on the earth's surface is still a significant challenge due to the lack of continuous and high-resolution spatial data. This issue has been particularly noted for observations of surface convective wind gusts over the ocean like the Gulf of Guinea, where the installation of the high-frequency radars and buoys for in-situ measurements remains very complicated.

Priftis *et al.* [11] and Kilpatrick and Xie [12] proposed ASCAT scatterometers for observations of surface winds associated with deep convection; however, they have not highlighted the process gathering the observations from multisatellites. In addition, the ASCAT scatterometers could not observe the most intense convective winds at a small scale due to their coarse spatial resolution. However, La *et al*. [13]–[16] suggested that synthetic aperture radar (SAR), especially *C*-band Sentinel-1 low earth orbit (LEO) satellites, could observe surface wind patterns associated with deep convection at both mesoscale and submesoscales. They also illustrated a strong relationship

Manuscript received August 5, 2021; revised September 23, 2021 and October 13, 2021; accepted November 8, 2021. Date of publication November 11, 2021; date of current version December 1, 2021. This work was supported in part by the Center National d'Etudes Spatiales in the framework of the Plateforme d'Exploitation des Produits Sentinel Program and in part by the BPI France. *(Corresponding author: Tran Vu La.)*

The authors are with the B-SPACE, Brest 29200, France (e-mail: tranvulaa@yahoo.com; christophe.messager@exwexs.fr).

Digital Object Identifier 10.1109/JSTARS.2021.3127401

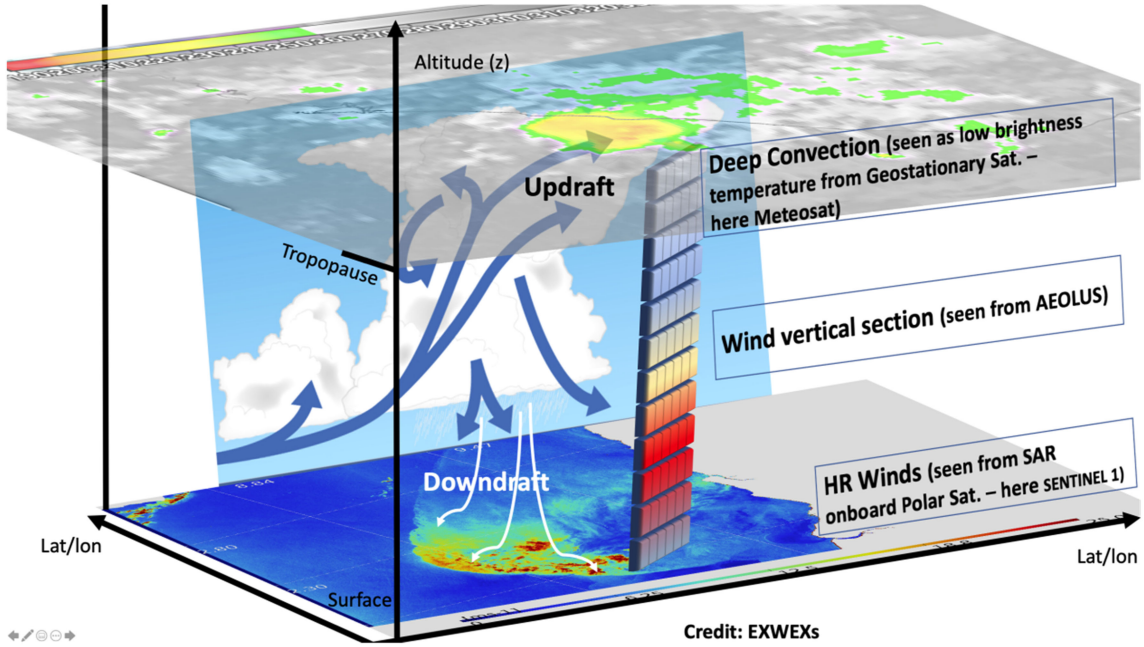

Fig. 1. 3-D view of a CS based on the combination of LEO and GEO satellites: the coldest deep convection at the tropopause altitude observed by Meteosat (GEO), intense downdrafts at the mid-levels (respective updrafts to balance the CS internal dynamics) detected by Aeolus (LEO), and the associated wind patterns at the sea surface observed by Sentinel-1 (LEO). Reproduced from [16].

between deep convective clouds observed by Meteosat and high-resolution surface winds on Sentinel-1 images. This assumption was completed in [16] by the combination of three different LEO and GEO satellites (Sentinel-1, Aeolus, and Meteosat) for the observation of deep convective clouds (200–230 K) aloft intense wind downdrafts (40 m/s) at the mid-levels, and intense wind patterns (12–25 m/s) at the sea surface. Such a combination thus offered a multiview [nearly three-dimensional (3-D)] of a CS as illustrated in Fig. 1(reproduced from [16]).

1) Deep convective clouds in their mature or developing stages are observed by the Meteosat GEO devices, for instance.
2) Intense upward/downward air fluxes generated by the deep convective clouds are measured by the Aeolus Lidar.
3) Regarding the downward air flux only, the so-called downdraft may become intense enough to reach and hit the sea surface, and that process may induce high surface wind gusts (exceeding 25–30 m/s) which can be estimated from Sentinel-1 SAR measurements.

Fig. 2 presents two cases of mesoscale wind gusts associated with deep convection observed on Sentinel-1 images offshore Nigeria, April 9, 2021 [see Fig. 2(a)], and offshore Ghana, May 6, 2021 [see Fig. 2(b)]. These cases illustrate high-intensity radar backscattering areas (in linear) associated with wind gusts induced from the hitting of intense convective downdrafts at the sea surface. The surface wind gusts in Fig. 2 tend to spread westward.

There are other assumptions in the literature to interpret the high-intensity radar backscattering areas from Sentinel-1 images as rainfall effects on the sea surface [17] or hydrometeors in the lower atmosphere [18]. However, as indicated in [19] and [20], the rainfall effects on radar backscattering at *C*-band are only significant for low wind speed (below 7 m/s). Therefore, under deep convection, where the associated surface wind gusts are much larger, the high-intensity radar backscattering areas detected on Sentinel-1 images should be mainly due to strong surface winds.

Inspired by some previous studies [13]–[16], the new and complementary results are presented here. They are based on the combination of LEO and GEO satellites to observe deep convection and the associated surface wind patterns through four combination scenarios as follows.

The first one combines Sentinel-1 (LEO) and Meteosat (GEO) to estimate convective wind gusts (Sentinel-1) and to detect the corresponding deep convective clouds (Meteosat) in the Gulf of Guinea. Thanks to the high spatial resolution and a wide swath of Sentinel-1 images, one can observe surface wind patterns at different scales (mesoscale and submesoscale), especially the wind hot-spots up to 25 m/s. The second one presents the combination of three satellites (Sentinel-1 LEO, Aeolus LEO, and Meteosat GEO) to obtain a multiview of deep convection, as illustrated in Fig. 1. The third one combines the *L*-band soil moisture active passive (SMAP) radiometer (LEO), Aeolus (LEO), and Meteosat (GEO) for observations of deep convection and convective surface wind patterns. The SMAP radiometer estimates sea surface wind speed based on differences between the SMAP-measured ocean surface brightness temperatures and the ones of the flat ocean surface. The SMAP measured input parameters differ from those of the method using SAR radar backscattering to retrieve sea surface wind speed. Furthermore, the *L*-band radar signal is much less impacted by precipitation, even under heavy rainfall [19], [21]. Finally, we combine four different satellites (Sentinel-1, SMAP, Aeolus, and Meteosat) to observe deep convection, intense wind downdrafts, sea surface

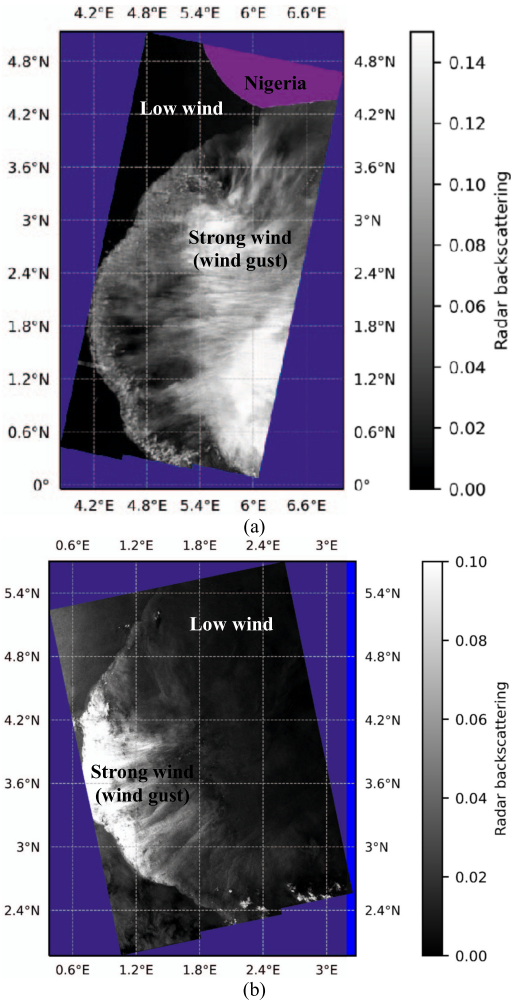

Fig. 2. Sentinel-1 images illustrate the high-intensity radar backscattering (in linear) associated with severe convective wind gusts moving westwards. These strong surface winds are induced when intense convective downdrafts hit the sea surface. (a) April 9, 2021, 05:22:22-05:23:40 UTC, offshore Nigeria (three images are gathered here from 05:22:22 to 05:23:40 UTC). (b) May 6, 2021, offshore Ghana (two images are gathered here from 18:09:10 to 18:10:04 UTC).

wind patterns, and the horizontal displacement of the latter by a combination of Sentinel-1 and SMAP.

The current study focuses on the region of the Gulf of Guinea (see Fig. 3) since it is one of the world regions where the CSs are the most numerous and intensive throughout the year, whatever the west African monsoon phase (meridional displacement of the CS activity area). In the meantime, it is a region with lots of human activities, and the CS hazards can trigger many disasters in terms of materials and human lives.

The rest of this article is organized as follows. Section II presents the methodology of this article, including data preparation, the combination of LEO and GEO satellites with a short time lag between them, and the methods of surface wind speed estimation from Sentinel SAR and SMAP radiometer data. Section III illustrates the multiview of CSs by the combination of LEO and GEO satellites. Finally, Section IV presents the discussion and conclusion.

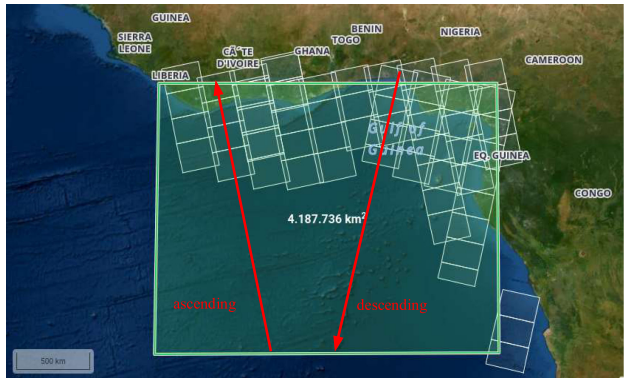

Fig. 3. Gulf of Guinea imaged by Sentinel-1A/B (ascending and descending orbit directions) from May 1 to 10, 2021. (Credit: EXWEXs).

II. Methodology

A. Data Preparation

Three LEO satellites (Sentinel-1, SMAP, and Aeolus) and one GEO (Meteosat) database are used to observe deep convection and surface wind patterns. Fig. 3 shows the Gulf of Guinea imaged by Sentinel-1A/B with the ascending (around 05:00-06:00 UTC) and descending (around 18:00-19:00 UTC) orbit directions. The two moments of observations correspond to the peaks of intense diurnal convection (late afternoon) over this region [22]. The large Sentinel-1 footprints enable the detection of surface wind patterns at the mesoscale. Sentinel-1 data acquired at level-1 are preprocessed to obtain radar backscattering, as shown in Fig. 2. It will be used in a geophysical model function (GMF) to retrieve surface wind speed.

SMAP mission was launched by NASA on January 29, 2015, to measure soil moisture and provide freeze/thaw classification for hydrology and carbon cycle studies. In addition, the SMAP radiometer measures ocean surface salinity and strong sea surface winds, specifically ocean winds within storms (e.g., CS) [21], [23]. The retrieved SMAP wind speeds are resampled over a 0.25° spatial grid following the method previously detailed in [24] to observe surface wind patterns associated with deep convection. SMAP passes over the Gulf of Guinea twice a day at around 06:00 UTC (descending direction) and 18:00 UTC (ascending direction). These periods correspond to the Sentinel-1 ones, and that facilitates the collocation of Sentinel-1 and SMAP data to observe the evolution of surface convective wind patterns, as presented in [14].

The Aeolus satellite was launched by the European Space Agency on August 22, 2018. It is the first mission to acquire profiles of Earth's wind on a global scale [25]. This article uses Aeolus data to detect intense vertical wind downdrafts associated with deep convection from the tropopause (about 17-km height) to the near ocean surface layers. As shown in Fig. 5–7, the wind updrafts and downdrafts are represented by the positive (+) values in blue and negative (–) ones in red, respectively. The more positive or negative the vertical wind values, the more intense the updrafts and downdrafts become. The missing data are due to dense water clouds. Aeolus passes over the Gulf of Guinea twice a day at around 05:00-06:00 UTC and 17:30-18:30

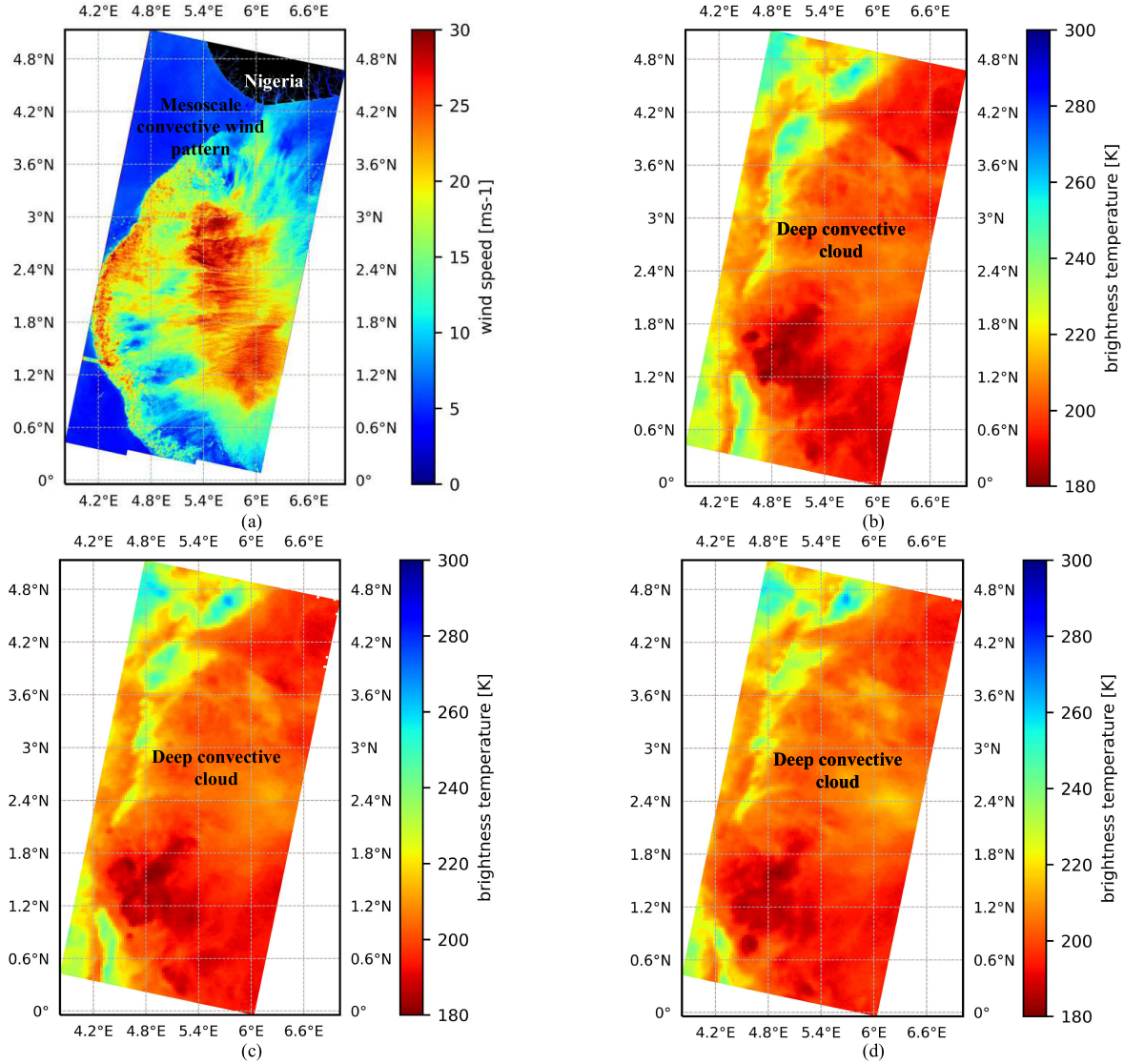

Fig. 4. Mesoscale surface wind pattern associated with deep convection offshore Nigeria, April 9, 2021. (a) Surface wind speed estimated from Sentinel-1 images, 05:22:22-05:23:40 UTC. (b)–(d) Corresponding deep (cold) convective clouds (180-200 K brightness temperature) observed by Meteosat at 05:06, 05:21, and 05:36 UTC, respectively.

UTC. These periods are close to the Sentinel-1 observation time. The accuracy of Aeolus vertical wind measurements has been studied in [26] and [27]. They are similar to the other wind observations in some cases and need to be improved in others. However, the Aeolus gives relevant qualitative information, and the acquired data are reliable to identify the intense downdrafts associated with deep convection as presented in this article.

The Meteosat series of satellites are GEO meteorological satellites operated by the EUMETSAT. They offer image data with a 2.8 km spatial resolution over Africa (Meteosat-9/10/11) every 15 min. The Meteosat short resampling time enables combinations with the LEO satellites (Sentinel-1, SMAP, Aeolus) to identify the relationship between deep convective clouds and surface wind patterns. In this article, we use the Meteosat SEVIRI image data–0° (channel 10–IR 12.0) to detect deep convective clouds with low brightness temperatures of 200–230 K. The Meteosat data are resampled on the grids of Sentinel-1 to ease comparisons between them.

B. Collocation of LEO and GEO Satellite Data

The combination of LEO and GEO satellites potentially allows observing deep convection and its vertical and horizontal dynamics. However, due to differences in orbit ephemeris, it is not easy to identify and collect relevant convective events both exhibited with LEO and GEO devices. For instance, from April to July 2020, we identified 17 time and location matching cases between Sentinel-1, Aeolus, and Meteosat over the Gulf of Guinea.

Table I gives four of the studied matching cases that allow observing surface wind patterns, intense air flux with downdrafts in the middle layer of the atmosphere, and deep convective

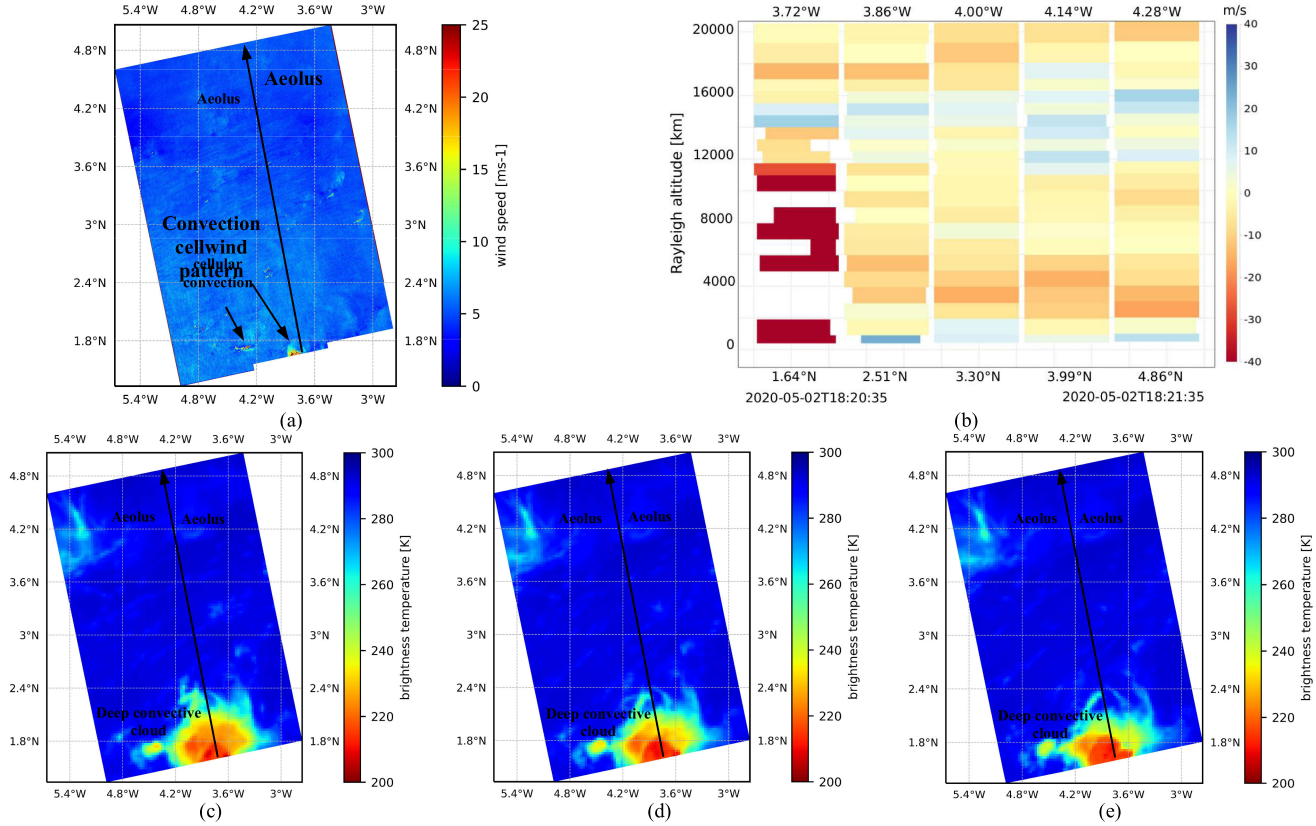

Fig. 5. Multiview of a submesoscale CS offshore Ivory Coast based on the combination of Sentinel-1, Aeolus, and Meteosat, May 2, 2020. (a) Surface wind pattern on Sentinel-1 images, 18:33:35-18:34:29 UTC. (b) Vertical cross-section wind intensity measured by Aeolus Lidar (18:20:35-18:21:35 UTC) corresponding to Sentinel-1 images (missing data are due to dense water clouds). (c)–(e) Corresponding deep (cold) convective clouds (200−220 K brightness temperature) observed by Meteosat at 18:21, 18:36, and 18:51 UTC, respectively.

TABLE I
COMBINATION OF LEO AND GEO SATELLITES FOR CS OBSERVATIONS

Case	Satellite	Time acquisition (UTC)	
#1	Sentinel-1	April 9, 2021	05:22:22-05:23:40
	Meteosat		05:06-05:36
#2	Sentinel-1	May 2, 2020	18:33:35-18:34:29
	Aeolus		18:20:35-18:21:35
	Meteosat		18:21-18:51
#3	SMAP	April 28, 2021	17:42-17:46
	Aeolus		17:38:00-17:41:15
	Meteosat		17:36-18:21
#4	Sentinel-1	May 6, 2021	18:09:10-18:10:04
	SMAP		17:45
	Aeolus		17:53:30-17:54:45
	Meteosat		17:36-18:21

clouds. The observation time differences in these cases do not exceed 15 min. The first case (#1) combines Sentinel-1 and Meteosat data with a 1-min time lag between them. The second case (#2) shows the combination of Sentinel-1, Aeolus, and Meteosat data, with (about) 13 min time difference between Sentinel-1 and Aeolus samples. The third case (#3) combines SMAP, Aeolus, and Meteosat data, with about 4 minutes time lag between SMAP and Aeolus data. Finally, last case (#4) presents the combination of Sentinel-1, SMAP, Aeolus, and Meteosat data, with a maximum of (about) 16 min time difference between Sentinel-1 and Aeolus samples.

C. Ocean Surface Wind Speed Estimation

Ocean surface wind patterns associated with deep convection can be detected on Sentinel-1 images as illustrated in [13]–[16]. This assumes that the convective downdrafts modify significantly sea surface roughness when they hit the sea surface. The surface roughness can be observed on the high-resolution SAR images as high-intensity radar backscattering areas (see Fig. 2). Therefore, convective wind gusts can be retrieved from Sentinel-1 data through the CMOD5.N GMF [28]. The CMOD5.N can estimate surface wind speed up to 25 m/s [29], [30] close to the convective wind intensity reported in [31]–[34].

Also, sea surface wind speed can be retrieved from the L-band SMAP-measured ocean surface brightness temperatures. For that, Meissner *et al.* [21] took the differences between the measured brightness temperatures and those of an idealized flat ocean surface and then used these differences within the radiative transfer model (RTM) that deduces, by inversion, corresponding surface wind speeds. The RTM processes are close to the CMOD5.N function, although the input parameters are different (ocean surface brightness temperature versus radar backscattering). Note that the SMAP-based wind data

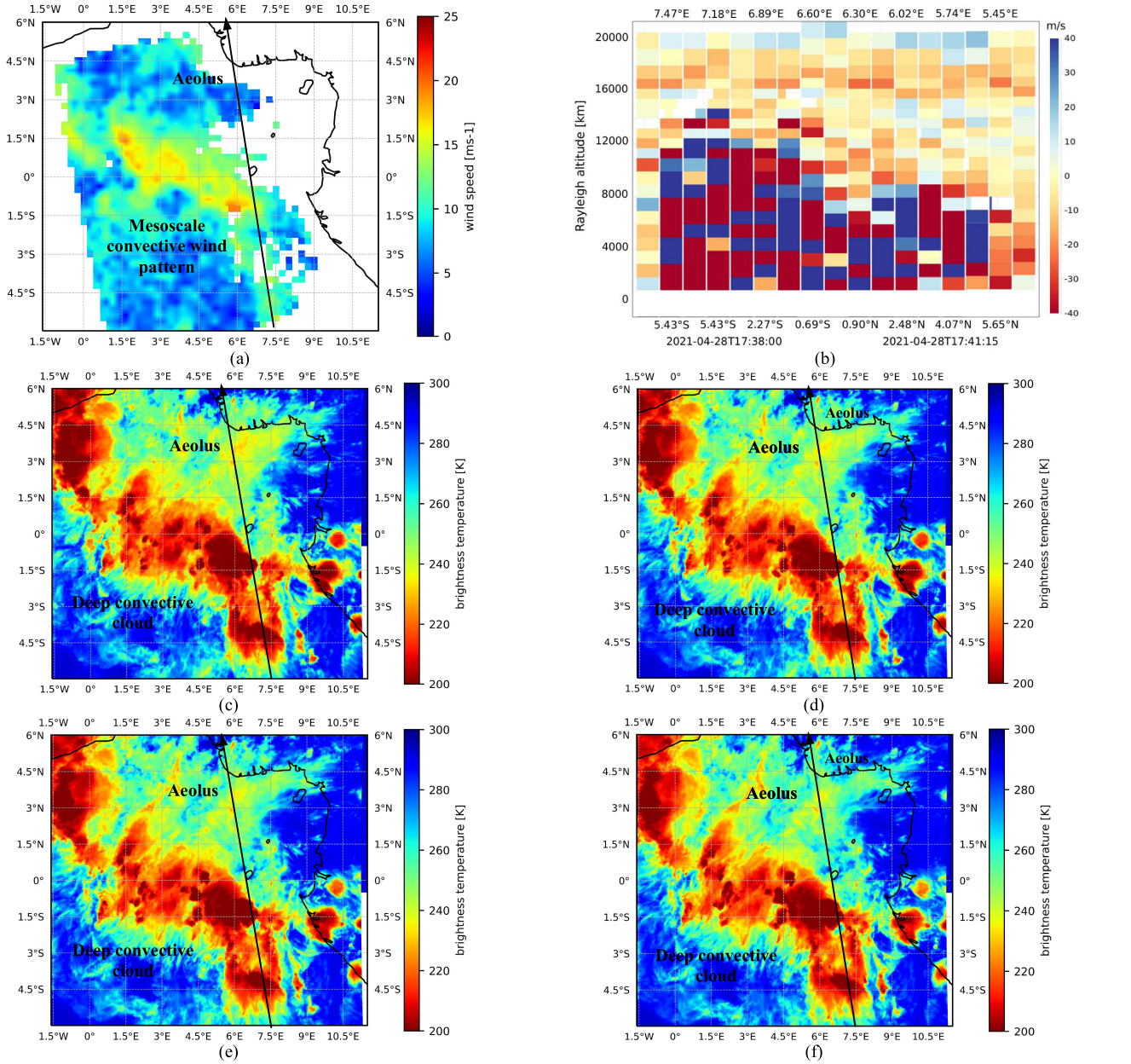

Fig. 6. Multiview of a huge mesoscale CS over the Gulf of Guinea based on the combination of SMAP, Aeolus, and Meteosat, April 28, 2021. (a) Surface wind pattern on SMAP image, 17:42-17:46 UTC. (b) Vertical cross-section wind intensity measured by Aeolus Lidar (17:38:00-17:41:15 UTC) corresponding to SMAP image. (c)–(f) Corresponding deep (cold) convective clouds (200−220 K brightness temperature) observed by Meteosat at 17:36, 17:51, 18:06, and 18:21 UTC, respectively.

are recommended for winds greater than 12 m/s, so it is well designed for strong wind estimation.

III. Multisatellites-Based CS Observation Case Study

A. Case #1 Based on Sentinel-1 and Meteosat Images

Case #1, April 9, 2021 (see Fig. 4) is a mesoscale strong surface wind pattern observation from Sentinel-1 images while the corresponding deep convective cloud is observed by Meteosat. Both features have close locations, especially when comparing Fig. 4(a) and (c) with only a 1-minute time lag. The wind pattern with 15-30 m/s [see Fig. 4(a)] is estimated from the radar backscattering shown in Fig. 2(a). These wind intensities are close to the convective wind gust magnitudes obtained by the coastal radars [32], small-scale NWP models [33], and *in situ* observations [34] under the similar weather conditions. Thanks to the wide Sentinel-1 footprint in Fig. 4(a) (gathering of three images), one can observe the wind pattern with 5° meridional spreading (roughly 550 km) which matches the coldest (deepest) convective cloud sections (180–200 K brightness temperature) through the Meteosat image in Fig. 4(c). In addition, when comparing Fig. 4(b)–(d), one notes that the deep convection moves westwards with the same direction as it may be assumed for surface wind pattern. The combination of LEO (Sentinel-1)

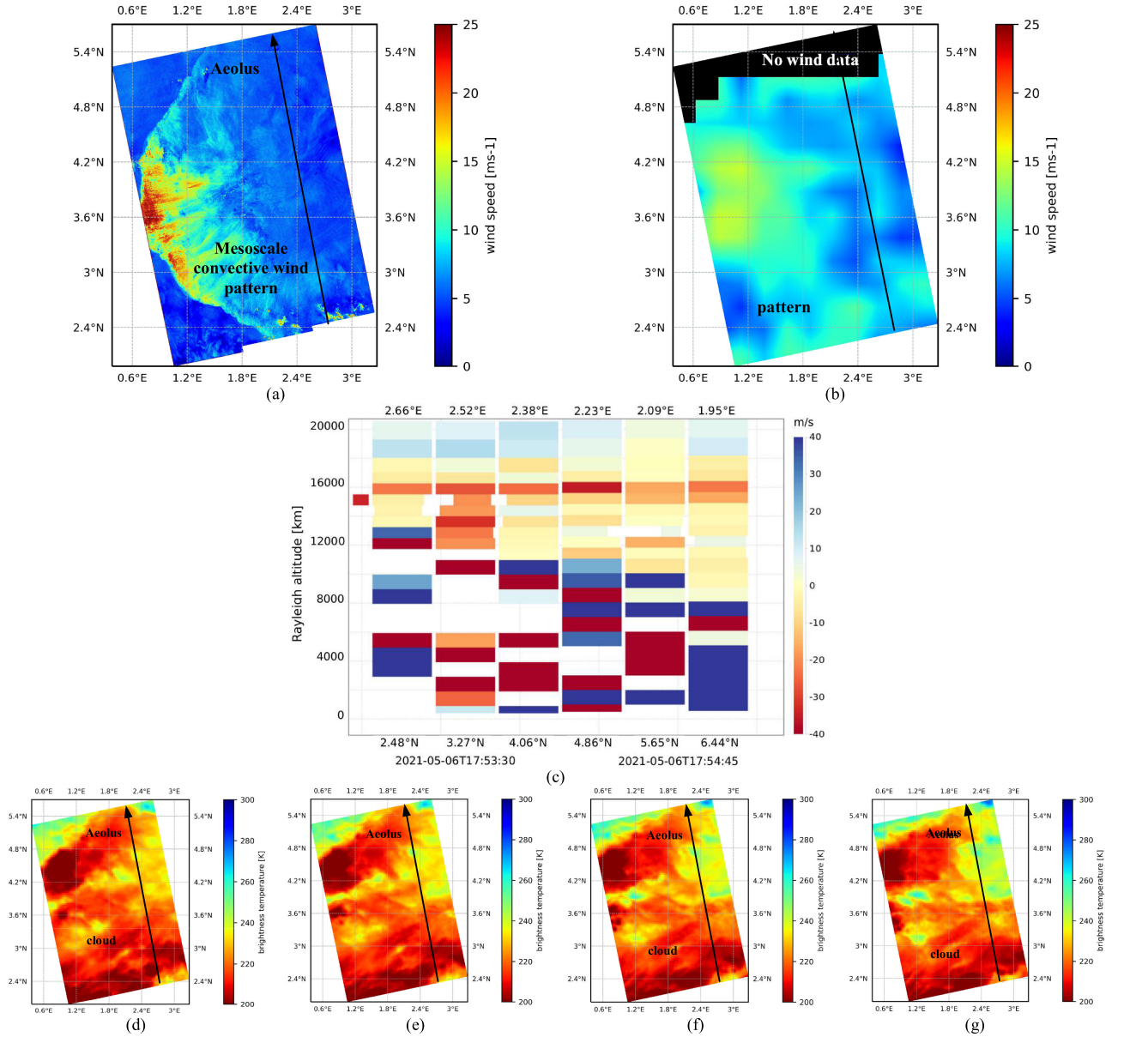

Fig. 7. Multiview of a huge mesoscale CS offshore Ghana based on the combination of Sentinel-1, SMAP, Aeolus, and Meteosat, May 6, 2021. (a) Surface wind pattern on Sentinel-1 images, 18:09:10-18:10:04 UTC. (b) Surface wind pattern on SMAP image, 17:45 UTC. (c) Vertical cross-section wind intensity measured by Aeolus Lidar (17:53:30-17:54:45 UTC) corresponding to SMAP image. (d)–(g) Corresponding deep (cold) convective clouds (200−220 K brightness temperature) observed by Meteosat at 17:36, 17:51, 18:06, and 18:21 UTC, respectively.

and GEO (Meteosat) satellites here facilitates the link identification between deep convective clouds and strong surface winds. However, it misses a vertical link at the mid-levels to connect the two events.

B. Case #2 Based on Sentinel-1, Aeolus, and Meteosat Images

Case #2, May 2, 2020 (see Fig. 5) is a multiview of a convection cell by a combination of Sentinel-1, Aeolus, and Meteosat images. Fig. 5(a) shows a small wind pattern on Sentinel-1 images having close locations to the deep convective clouds (200-220 K brightness temperature) detected by Meteosat [see Fig. 5(c)–(e)]. The coldest cloud areas correspond to the strongest surface winds. In particular, when comparing Fig. 5(a), (b), and (d), one notes a good agreement in the location of the three processes: a pattern of high winds over the sea surface, an intense downdraft (−40 m/s) at the mid-levels up to the surface, and a deep convective cloud aloft. The vertical cross-section wind profile measured by Aeolus [see Fig. 5(b)] illustrates a connection between the two processes observed by Sentinel-1 and Meteosat. It represents a typical powerful downward air flux associated with deep convection. The updrafts (+20–30 m/s) are detected at the 14–15 km heights. These air parcels become colder and denser, they then move downward and form the

so-called downdrafts. When these intense downdrafts hit the sea surface, they induce strong horizontal surface winds (or wind gusts) exceeding 25 m/s, as shown in Figs. 4 and 5.

Case #2 illustrates a significant advantage of the LEO and GEO satellite combinations for the CS observations. It exhibits the dynamical link of the three processes observed by Sentinel-1, Aeolus, and Meteosat. This case also illustrates the sensitivity of the three devices for the multiview of deep convection at various scales (cellular convection, submesoscale, and mesoscale CS).

C. Case #3 Based on SMAP, Aeolus, and Meteosat Images

Case #3, April 28, 2021 (see Fig. 6) presents a combination of SMAP, Aeolus, and Meteosat images for a mesoscale CS observation. Fig. 6(a) illustrates surface wind speeds estimated from the SMAP-measured ocean surface brightness temperatures. They are resampled on the Meteosat grid at a 2.8 km horizontal resolution. The sea surface wind pattern on the SMAP image (15–20 m/s wind intensity) spreads meridionally and zonally over about 3° and 4.5°, respectively, (1.5°S–1.5°N, 1.5°E–6°E). The SMAP strongest surface wind pattern is closely located to the deep convective clouds detected by Meteosat, especially at 17:36 [see Fig. 6(c)] and 17:51 UTC [see Fig. 6(d)]. In particular, the coldest cloud parts (200 K, or less) match the wind hot-spots (about 18–20 m/s). Such a result has also been noted when comparing Sentinel-1 surface wind patterns and deep convective clouds. However, compared to case #1 (see Fig. 4), it is hard to isolate a clear squall front, thus it is not possible to assume a surface wind feature displacement direction for the SMAP wind pattern. Likewise, it is difficult to determine the displacement direction of the deep convective cloud cells since they are located at the same position for 45 min (17:36-18:21 UTC).

Fig. 6(b) presents the vertical cross-section winds observed by Aeolus at the location close to the SMAP [see Fig. 6(a)] and Meteosat [see Fig. 6(c)–(f)] images. They show the vertical dynamics of deep convection, including intense updrafts and downdrafts at the mid-levels. In particular, some strong downdrafts are noted near the sea surface, and they likely induce the large surface wind pattern observed on the SMAP image, especially at (1.48°S, 6.74°E) where the intense downdrafts match strong surface winds, as shown in Fig. 1 and in [16].

Despite a coarse spatial resolution and validation for only winds above 12 m/s [24], one can observe surface wind patterns under deep convection based on the SMAP ocean wind speed estimates. The SMAP-estimated convective wind intensity is very close to that retrieved from Sentinel-1 data (about 15–20 m/s), and it is relevant with the magnitudes of the convective wind gusts indicated in [31]–[34]. Therefore, the SMAP-based wind data may be used with the Aeolus and Meteosat data for the multiview of deep convection at mesoscale. In particular, a combination of Sentinel-1 and SMAP with a short time lag enables observations of the displacement direction of surface wind patterns that has not been studied yet in the literature.

D. Case #4 Based on Sentinel-1, SMAP, Aeolus, and Meteosat

Case #4, May 6, 2021 (see Fig. 7) illustrates a combination of Sentinel-1, SMAP, Aeolus, and Meteosat for a multiview of a mesoscale CS. Fig. 7(a) presents a mesoscale surface wind pattern (15–25 m/s) obtained from the Sentinel-1 radar backscattering [see Fig. 2(b)]. It spreads meridionally over more than 3° (2.4°N–5.4°N) and is assumed to move southwestwards based on the front of the wind pattern (high wind intensity). Fig. 7(b) shows the same surface wind pattern as Fig. 7(a), but retrieved from the SMAP data acquired 15 min before the Sentinel-1 image. The SMAP-observed convective winds (about 15–17 m/s) do not exhibit wind hot spots due to the SMAP coarse spatial resolution. Although it is not easy to determine the region with strong wind gradients on the SMAP image, one may assume that the surface wind pattern moves southwestwards when comparing Fig. 7(a) and (b). It is worth noting that the wind patterns in Fig. 7(a) and (b) are closely compared to the deep convective clouds detected by Meteosat at 17:51 UTC [see Fig. 7(e)] and 18:06 UTC [see Fig. 7(f)]. When comparing the Meteosat images from 17:36 to 18:21 UTC [see Fig. 7(d)–(g)], one can note that deep convective clouds tend to move southwestward as well. This observation is more evident when we note the change of the coldest cloud patterns (about 200 K). This result then leads to assume that deep convective clouds and surface wind patterns have the same displacement direction (southwestward).

Fig. 7(c) presents the Aeolus vertical cross-section wind profiles aloft the same horizontal Sentinel-1 and SMAP footprint images [see Fig. 7(a) and (b)]. They illustrate the vertical dynamics of deep convection, including intense updrafts and downdrafts. The Aeolus footprint is located on the east of the intense surface wind patterns. In practice, it is not easy to collect simultaneously three observations based on the combination of LEO and GEO satellites due to observation time lags; however, it is possible to accept a time lag if it is still small compared to the convection development rate time. One can note that the Aeolus convective vertical winds in Fig. 7(c) may be associated with the large deep convective clouds [see Fig. 7(d)–(g)]. Likewise, they match the surface wind patterns in Fig. 7(a) and (b). This assumes that the Aeolus intense downdrafts may induce surface wind patterns moving southwestwards and being detected by Sentinel-1 and SMAP.

IV. Discussion, Conclusion, and Perspective

This article combined observations from three LEO (Sentinel-1, SMAP, and Aeolus) and one GEO (Meteosat) satellite to observe some CSs and their associated vertical and horizontal dynamics. This offers advantages to observe, monitor, and understand deep convection. These advantages can be listed, as follows.

First, the combination of Sentinel-1 and (or) SMAP with Aeolus and Meteosat strengthened the schematic understanding of deep convection as illustrated in Fig. 1: the warm air associated with the intense updrafts (observed by Aeolus) contributes to the ignition and development of deep convective clouds (observed by Meteosat). The warm air is then cooled as it rises and becomes heavier, and finally moves back towards the surface as downdraft. If it is intense enough, it can be measured by Aeolus, as shown in Figs. 5(b), 6(b), and 7(c). When the downdraft hits

the sea surface, it can induce wind gusts detectable by Sentinel-1 and SMAP via radar backscattering and ocean surface brightness temperatures, respectively [see Figs. 4(a)–7(a)].

Second, the simultaneous observations by the LEO and GEO satellites strengthened the assumption that the high-intensity radar backscattering (see Fig. 2) is induced by strong surface winds associated with deep convection rather than by some other effects like hydrometeors in the melting layer [18] or precipitation [17] at the sea surface. It is even more significant when a combination of Sentinel-1 and SMAP surface wind retrieval is used. Indeed, the two devices (Sentinel-1 and SMAP) use different estimation methods of sea surface wind speed but give similar surface wind patterns associated with deep convection. Moreover, the combination of the two wind data sources enables the observation of displacement direction of the surface wind patterns in accordance with the deep convective cell displacement.

Third, the high spatial resolution of Sentinel-1 permits the observation of more small-scale details and thus more powerful dynamics scales such as submesoscale. As a result, it is easier to highlight the location of the highest wind areas as the region with strong wind gradients of a CS [see Figs. 4(a) and 7(a)]. Likewise, the gathering of several concomitant Sentinel-1 images, as shown in Fig. 2, enables the observations of the region with strong wind gradients. Despite having a coarse spatial resolution, SMAP data can be used as a complementary source to observe convective wind gusts [see Figs. 6(a) and 7(b)], particularly over the open sea where Sentinel-1 data are not available.

Fourth, the combination of LEO and GEO satellites proposed some perspectives to improve the forecast of convective wind gusts that have not been carried out by most NWP models. Likewise, one can apply machine learning/deep learning on the available database having the matching of the three types of observations from Sentinel-1/SMAP, Aeolus, and Meteosat, to explore the relationships between deep convective clouds and surface wind patterns. Also, the learning models may be used to forecast the occurrence and magnitudes of strong surface winds under convective clouds observed from only the GEO data without the additional Sentinel-1 and/or SMAP data.

Some limitations regarding the developed methodology in this article should be mentioned. To estimate surface wind speeds, this article used wind directions extracted from the ERA5 data [35] as input of CMOD5.N. However, ERA5 is not based on an eddy-permitted model and is not able to resolve explicitly the convection processes, and as a result, one can argue that the use of ERA5 may lead to some bias in the estimation of convective wind. Therefore, the correction of surface wind directions associated with deep convection should be one of the improvements that could be addressed afterward. Also, CMOD5.N has been studied with a hypothesis of the atmospheric stability conditions, while deep convection generates large instabilities. This may lead to errors in wind speed estimation as well.

The Aeolus measurements, as indicated in [26] and [27], may produce some errors in vertical wind intensity compared to the other sources. The data calibration of the Rayleigh and Mie channels should thus be improved for new versions. However, this issue did not impact significantly the location matching between deep convective clouds detected by Meteosat, intense downdrafts observed by Aeolus, and surface wind patterns on Sentinel-1 images.

The observation time lag between the three satellite devices (Sentinel-1/SMAP, Aeolus, and Meteosat) is an important parameter to evaluate the process matching between deep convective clouds, intense downdrafts, and surface wind patterns. In general, the time lag below 15 min allows a standard interpretation of the three observations as part of a single CS phenomenon. However, it should be relevant to study more cases of observation time lag, especially short and moderate time, to evaluate more deeply the relationship between deep convective clouds and surface wind patterns, which is highly significant for convective wind gust forecast.

ACKNOWLEDGMENT

Sentinel-1A/B images are given by the European Copernicus Program. Meteosat images are provided by the European Organization for the Exploitation of Meteorological Satellites (EUMETSAT) via EUMETSAT Data Center. Aeolus data are downloaded via the virtual research platform VirES.[1] SMAP wind data are given.[2] The ERA5 data are obtained.[3] The authors would like to thank the Reviewers and the Editors of the journal for the constructive comments.

REFERENCES

[1] S. Mohr, M. Kunz, A. Richter, and B. Ruck, "Statistical characteristics of convective wind gusts in Germany," *Nat. Hazards Earth Syst. Sci.*, vol. 17, pp. 957–969, Jun. 2017.

[2] S. J. Kastman, S. P.Market, I. N. Fox, A. L. Foscato, and R. A. Lupo, "Lightning and rainfall characteristics in elevated vs. surface based convection in the midwest that produce heavy rainfall," *Atmosphere*, vol. 8, no. 2, Feb. 2017.

[3] V. Mathon and H. Laurent, "Life cycle of Sahelian mesoscale convective cloud systems," *Quart. J. Roy. Meteorol. Soc.*, vol. 127, pp. 377–406, 2001.

[4] L. A. T. Machado, W. B. Rossow, R. L. Guedes, and A. W. Walker, "Life cycle variations of mesoscale convective systems over the Americas," *Monthly Weather Rev.*, vol. 126, no. 6, pp. 1630–1654, 1998.

[5] L. A. T. Machado, H. Laurent, and A. A. Lima, "Diurnal March of the convection observed during TRMM-WETAMC/LBA," *J. Geophys. Res. (Atmos.)*, vol. 107, no. D20, 2002.

[6] J. M. Sieglaff, L. M. Cronce, W. F. Feltz, K. M. Bedka, M. J. Pavolonis, and A. K. Heidinger, "Nowcasting convective storm initiation using satellite-based box-averaged cloud-top cooling and cloud-type trends," *J. Appl. Meteorol. Climatol.*, vol. 50, no. 1, pp. 110–126, Jan. 2011.

[7] J. Sun *et al.*, "Use of NWP for nowcasting convective precipitation: Recent progress and challenges," *Bull. Amer. Meteorol. Soc.*, vol. 95, no. 3, pp. 409–426, Mar. 2014.

[8] L. M. V. Carvalho and C. Jones, "A satellite method to identify structural properties of mesoscale convective systems based on the maximum spatial correlation tracking technique (MASCOTTE)," *J. Appl. Meteorol.*, vol. 40, no. 10, pp. 1683–1701, 2001.

[9] Aug. 2021. [Online]. Available: https://www.goes-r.gov/spacesegment/abi.html

[10] Aug. 2021. [Online]. Available: https://www.eumetsat.int/meteosat-third-generation

[11] G. Priftis, T. J. Lang, and T. Chronis, "Combining ASCAT and NEXRAD retrieval analysis to explore wind features of mesoscale oceanic systems," *J. Geophys. Res.. Atmos.*, vol. 123, no. 18, pp. 10341–10360, Sep. 2018.

[1] [Online]. Available: https://aeolus.services/

[2] [Online]. Available: www.remss.com/

[3] [Online]. Available: https://cds.climate.copernicus.eu/

[12] T. J. Kilpatrick and S-P. Xie, "ASCAT observations of downdrafts from mesoscale convective systems," *Geophys. Res. Lett.*, vol. 42, no. 6, pp. 1951–1958, Mar. 2015.
[13] T. V. La, C. Messager, M. Honnorat, and C. Channelliere, "Detection of convective systems through surface wind gust estimation based on Sentinel-1 images: A new approach," *Atmos. Sci. Lett.,* vol. 19, no. 12, Dec. 2018, Art. no. e863.
[14] T. V. La and C. Messager, "Convective system sea surface wind pattern detection and variability observation from a combination of Sentinel-1 and Radarsat-2 images," *Rem. Sens. Lett.*, vol. 11, no. 5, pp. 446–454, Feb. 2020.
[15] T. V. La *et al.*, "Use of Sentinel-1 C-band SAR images for convective system surface wind pattern detection," *J. Appl. Meteor. Climatol.,* vol. 59, no. 8, pp. 1321–1332, Aug. 2020.
[16] T. V. La and C. Messager, "Convective system dynamics viewed in 3D over the oceans," *Geophys. Res. Lett.*, vol. 48, Feb. 2021, Art. no. e2021GL092397.
[17] C. Nie and D. G. Long, "A C-Band wind/rain backscatter model," *IEEE Trans. Geosci. Remote Sens.*, vol. 45, no. 3, pp. 621–631, Mar. 2007, doi: 10.1109/TGRS.2006.888457.
[18] W. Alpers, Y. Zhao, A. A. Mouche, and P. W. Chan, "A note on radar signatures of hydrometeors in the melting layer as inferred from Sentinel-1 SAR data acquired over the ocean," *Remote Sens. Environ.*, vol. 253, Nov. 2020.
[19] R. F. Contreras and W. J. Plant, "Surface effect of rain on microwave backscatter from the ocean: Measurements and modeling," *J. Geophys. Res.*, vol. 111, no. C8, Aug. 2006, Art. no. C08019.
[20] F. Xu, X. Li, P. Wang, J. Yang, W. G. Pichel, and Y. Q. Jin,"A backscattering model of rainfall over rough sea surface for synthetic aperture radar," *IEEE Trans. Geosci. Remote*, vol. 53, no. 6, pp. 3042–3054, Jun. 2015, doi: 10.1109/TGRS.2014.2367654.
[21] T. Meissner, L. Ricciardulli, and F. J.Wentz, "Capability of the SMAP mission to measure ocean surface winds in storms," *Bull. Amer. Meteorol. Soc.*, vol. 98, no. 8, pp. 1660–1677, Aug. 2017.
[22] M. Lothon *et al.*, "Life cycle of a mesoscale circular gust front observed by a C-band Doppler radar in West Africa," *Monthly Weather Rev.*, vol. 139, no. 5, pp. 1370–1388, May 2011.
[23] S. H. Yueh *et al.*, "SMAP L-band passive microwave observations of ocean surface wind during severe storms," *IEEE Trans. Geosci. Remote Sens.*, vol. 54, no. 12, pp. 7339–7350, Dec. 2016, doi: 10.1109/TGRS.2016.2600239.
[24] Aug. 2021. [Online]. Available: https://www.remss.com/missions/smap/winds.
[25] A. Stoffelen *et al.*, "Wind profile satellite observation requirements and capabilities," *Bull. Amer. Meteorol. Soc.*, vol. 101, no. 11, pp. E2005–E2021, Nov. 2020.
[26] B. Witschas *et al.*, "First validation of aeolus wind observations by airborne Doppler wind lidar measurements," *Atmos. Meas. Tech.*, vol. 13, pp. 2381–2396, 2020.
[27] J. Guo *et al.*, "Technical note: First comparison of wind observations from ESA's satellite mission aeolus and ground-based radar wind profiler network of China," *Atmos. Chem. Phys.*, vol. 21, pp. 2945–2958, 2021.
[28] J. Verspeek, A. Stoffelen, M. Portabella, H. Bonekamp, C. Anderson, and J. FigaSaldaña, "Validation and calibration of ASCAT data using ocean backscatter and CMOD5.N," *IEEE Trans. Geosci. Remote Sens.*, vol. 48, no. 1, pp. 386–395, Jan. 2010, doi: 10.1109/TGRS.2009.2027896.
[29] T. V. La, A. Khenchaf, F. Comblet, and C. Nahum, "Exploitation of C-band Sentinel-1 images for high-resolution wind field retrieval in coastal zones (Iroise Coast, France)," *IEEE J. Sel. Topics Appl. Earth Observ. Remote Sens.*, vol. 10, no. 12, pp. 5458–5471, Dec. 2017, doi: 10.1109/JSTARS.2017.2746349.
[30] T. V. La, A. Khenchaf, F. Comblet, and C. Nahum, "Assessment of wind speed estimation from C-band Sentinel-1 images using empirical and electromagnetic models," *IEEE Trans. Geosci. Remote Sens.*, vol. 56, no. 7, pp. 4075–4087, Jul. 2018, doi: 10.1109/TGRS.2018.2822876.
[31] W. R. Cotton, G. Bryan, and S. C. van den Heever, "Storm and cloud dynamics – the dynamics of clouds and precipitating mesoscale systems, chapter 9 – mesoscale convective systems," in *International Geophysics*. Cambridge, MA, USA: Academic, 2011, pp. 455–526.
[32] P. F. Waniha, R. D. Roberts, J. W. Wilson, A. Kijazi, and B. Katole, "Dual-polarization radar observations of deep convection over Lake Victoria basin in east Africa," *MDPI Atmos.*, vol. 10, no. 11, Nov. 2019, Art. no. 706.
[33] J. M. Chamberlain, C. L. Bain, D. F. A. Boyd, K. McCourt, T. Butcher, and S. Palmer, "Forecasting storms over Lake Victoria using a high resolution model," *Meteorol. Appl.*, vol. 21, no. 2, pp. 419–430, Apr. 2014.
[34] M. Imberger, X. G. Larsén, and N. Davis, "Investigation of spatial and temporal wind-speed variability during open cellular convection with the model for prediction across scales in comparison with measurements," *Boundary-Layer Meteorol.*, vol. 179, pp. 291–312, 2021.
[35] H. Hersbach *et al.*, "The ERA5 global reanalysis," *Quart. J. Roy. Meteorol. Soc.*, vol. 146, pp. 1999–2049, 2020.

Tran Vu La (Member, IEEE) received the degree in electronics and telecommunications engineering from the HCMC University of Technology, Ho Chi Minh City, Vietnam, in 2008, and the M.Sc. degree in signal processing and telecommunication systems, and Ph.D. degree in design and optimization of high-gain dielectric lens antennas with reduced size in millimeter waves from the University of Rennes 1, Rennes, France, in 2009 and 2012, respectively.

From 2012 to 2014, he was a Post-Doctoral Researcher with IMT Atlantic (Telecom Bretagne), Brest, France. From 2014 to 2017, he was a Researcher with ENSTA Bretagne, Brest, France. From 2017 to 2021, he was with EXWEXs, Brest, France, as an R&D Engineer. He is currently with B-SPACE, Brest, France, as a Senior R&D Engineer. Currently, his research focuses on applying Artificial Intelligence (ML/DL) for Earth Observation. His research interests include Remote Sensing for EarthObservation (oceanography, meteorology, agriculture, sea ice, and environment), the processing of satellite images (SAR, optical, hyperspectral).

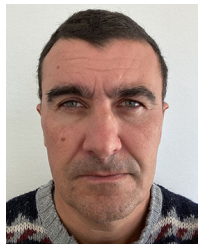

Christophe Messager received the Master's degree in meteorology and oceanography from the Université de Toulon et du Var, in 1994, the M.Sc. degree in physical oceanography from the Centre d'Océanologie de Marseille, in 1995, the Ph.D. degree in atmospheric science from the Université Joseph Fourier, in 2005, and then an "Habilitation à Diriger de Recherche—Accreditation to Supervise Research", Université de Bretagne Occidentale, in 2015.

He was the former Founder and the Head of the ICEMASA International French-South African Marine Laboratory, then the Head of the Laboratoire de Physique des Océans—Ocean Physics Laboratory until 2015. From spring 2012, he was the Founder of Extreme Weather Expertises company. In 2020, he founded the B-Space company for which he is also the leader. His research interests include atmospheric science, meteorology and climate, and especially convective systems and ocean-atmosphere interactions, as well as the applications of remote sensing in satellite meteorology and oceanography.